💬 COMMENTARY

# Visualizing the three-metal-ion-dependent cleavage of a mutagenic nucleotide

Nadine L. Samara[a,1] ⓘ

The accurate replication, transcription, and maintenance of genetic material requires housekeeping enzymes that prevent the spontaneous mutagenesis of DNA by catalyzing the removal of oxidized deoxynucleoside triphosphates (dNTPs). These include the Nudix hydrolase superfamily member human Mut1 homolog (MTH1, human NUDT1), which catalyzes the removal of a variety of oxidized dNTPs such as 8-oxo-dGTP, 2-oxo-dATP, and 8-oxo-dATP (1, 2). The Nudix hydrolases are divalent cation ($Mg^{2+}/Mn^{2+}$) dependent enzymes that have protective, regulatory, and signaling functions across all domains of life and share a Nudix box motif $GX_5EX_7REUXEEXGU$ (U is a bulky hydrophobic residue and X is any amino acid other than the essential glutamates) that forms the active site (1, 2). In addition to its role in DNA maintenance, MTH1 is up-regulated in many tumors and is a chemotherapeutic target. Thus, the architecture and catalytic mechanism of MTH1 have been of considerable interest. The most extensively characterized Nudix enzyme is *Escherichia coli* pyrophosphohydrolase MutT, a homolog of MTH1 that efficiently catalyzes the excision of an oxidatively damaged 8-oxo-dGTP to sanitize the nucleotide pool and avoid misincorporation of 8-oxo-G opposite dA during DNA replication (1). The reaction occurs via a nucleophilic attack at the β-phosphorus to convert 8-oxo-dGTP to a nucleotide monophosphate (NMP) and inorganic pyrophosphate. Kinetic and static structural studies of MutT show that the hydrolytic reaction may proceed via a two-metal-ion mechanism (1, 3–7). However, differences in substrate binding, metal coordination, and number of metals observed in the active site among the published structures leave unanswered questions about the MutT reaction pathway that are addressed by Nakamura and Yamagata in PNAS (8).

Inconsistencies among structures of similar enzyme–substrate (ES) complexes occur because catalytically inactive mutants or nonreactive substrate analogs are often used to obtain homogeneous, well-diffracting crystals or stable complexes for solution studies, which potentially perturb or misrepresent the biologically accurate active site configuration. Another downside of using static, nonreactive enzyme–substrate complexes is that these structures do not capture factors that appear during product formation, such as transient metals. The first solution structure of MutT in complex with $Mg^{2+}$ and a nonhydrolyzable adenosine analog AMPCPP showed that one metal coordinates and aligns the γ- and β-phosphates in 8-oxo-dGTP, and the second metal is coordinated by four active-site residues, Gly38, Glu56, Glu57, and Glu53 (9). X-ray crystal structures of MutT-$Mn^{2+}$ and MutT-8-oxo-dGMP-$Mn^{2+}$ revealed features similar to the solution structure but also exposed discrepancies (10). In both structures, Glu57 and Glu53 bind an active site metal, consistent with kinetic data showing that these two residues have the greatest catalytic defects when changed to Gln (11). However, the other metal-binding residues differ between the structures.

Gly38 coordinates metal in the solution structure, but Gly37 directly coordinates the metal in the crystal structure, while Gly38 is instead involved in β-sheet formation. In the solution structure, Glu56 and Glu98 directly coordinate metals, whereas in the crystal structures these residues interact with the waters that coordinate the active-site metals. The crystal structures also reveal three possible metal binding sites, with two metals observed in the MutT-$Mn^{2+}$ structure and one distinct metal site observed in the MutT-8-oxo-dGMP-$Mn^{2+}$ structure, alluding to the possibility that these enzymes use three metals for catalysis instead of two, in contrast to the earlier proposed two-metal-dependent models (2, 9, 11).
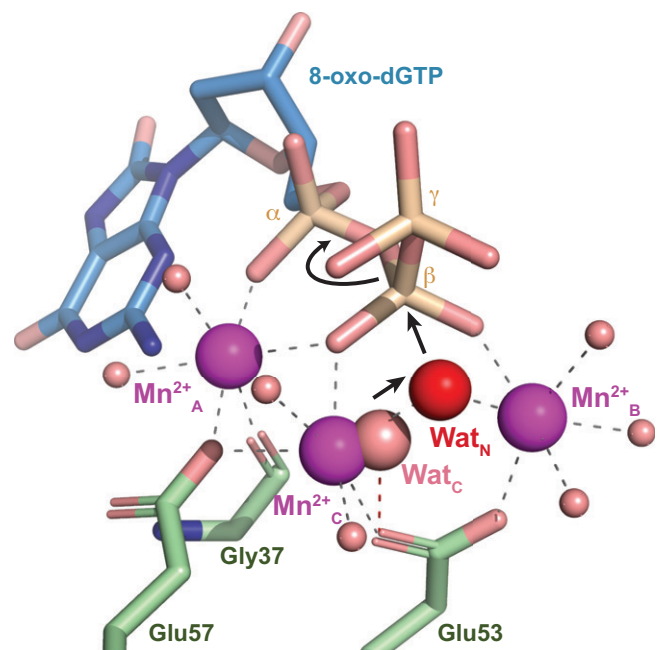


**Fig. 1.** The MutT active site in State 3 of catalysis. MutT active-site residues Glu57, Glu53, and Gly37 (green) coordinate three metal ions $Mn^{2+}_A$, $Mn^{2+}_B$, and $Mn^{2+}_C$ (magenta) that interact with and align 8-oxo-dGTP (blue) for catalysis. A possible path (black arrows) for nucleophile activation starts with $Wat_C$ (pink) coordination and deprotonation by Glu53 before it moves to a new location $Wat_N$ (red), which is coordinated by $Mn^{2+}_B$ and $Mn^{2+}_C$ and positioned for inline nucleophilic attack at the β-phosphorus.

Author affiliations: [a]Structural Biochemistry Unit, National Institute of Dental and Craniofacial Research, National Institutes of Health, Bethesda, MD 20892

Nakamura and Yamagata resolve these conflicts by using *in crystallo* catalysis and time-lapse crystallography to observe MutT catalyzed hydrolysis of the wild-type enzyme and its genuine substrate, the mutagenic nucleotide 8-oxo-dGTP, in the presence of divalent metal cations $Mn^{2+}$ or $Mg^{2+}$ (8). The enzyme–substrate complex was initially cocrystallized in the absence of $Mg^{2+}/Mn^{2+}$ and the reaction was initiated by soaking the crystals in solutions containing divalent cations at concentrations that support catalysis for discrete time periods and stopped by freezing (12). This was followed by classic X-ray crystallography, where X-ray diffraction data were collected at each reaction time point and trapped by freezing to visualize the reaction as it progresses over time. This protocol has successfully been applied to several polymerases and nucleases thus far to visualize the entire reaction time course, and in all cases additional metal ions (usually a third divalent cation, and occasionally monovalent $K^+$ ions as observed in the RNase H1 cleavage of RNA) transiently appear as the reaction proceeds to product formation. These cations help position the substrates and nucleophile and stabilize the reaction intermediate (13–21). Without the third divalent cation, product does not form (18, 22).

> ### *In crystallo* catalysis has unequivocally illustrated the ubiquitous role of three metal ions in reactions formally known for two-metal ion catalysis.

The authors have captured five distinct reaction states of MutT-catalyzed 8-oxo-dGTP hydrolysis and take advantage of the anomalous signal from $Mn^{2+}$ to track three distinct $Mn^{2+}$ cations that appear stepwise as the reaction proceeds, with the third metal reaching its maximum occupancy prior to nucleophilic attack and decreasing in intensity as substrate is converted to product. In State 1, $Mn^{2+}_A$ interacts with the α-phosphate of 8-oxo-dGTP, which otherwise adopts two conformations in the ES complex and in the absence of $Mn^{2+}_A$ to stabilize a single conformation. Two additional metals appear in State 2: $Mn^{2+}_B$, which helps to rotate and orient the γ-phosphate, and $Mn^{2+}_C$, which partially occupies a position that is overlapping with a water molecule coordinated to Glu53. In State 3, the occupancy of $Mn^{2+}_C$ is at its maximum, the occupancy of the water coordinated to Glu53 is reduced ($Wat_C$), and a new water appears between $Mn^{2+}_B$ and $Mn^{2+}_C$ ($Wat_N$). State 3 represents the active-site configuration prior to nucleophilic attack (Fig. 1) and has the highest anomalous signal for each of the three metals. In this state, the 8-oxo-dGTP is aligned for catalysis and $Wat_N$ coordinated by $Mn_B^{2+}$ and $Mn_C^{2+}$ is positioned for the in-line attack of the β-phosphorus in the 8-oxo-dGTP. Based on the solution structure, Lys39 was proposed to function as a Lewis acid that promotes the departure of NMP given its interactions with the leaving group, and the K39Q mutation decreases the first-order rate constant ($k_{cat}$) eightfold and eliminates the pH dependence of the reaction (9, 11). In State 4, Lys39 makes interactions with the γ-phosphate of 8-oxo-dGTP to align the substrate and neutralize charges that help promote product release. Overall, the *in crystallo* structures support the three-metal-ion-dependent mechanism, which is also consistent with previously published data from kinetics and mutational analyses (11).

One of the main questions addressed in the study is nucleophilic water deprotonation. Earlier kinetic studies proposed a role for Glu53 as the general base, supported by an E53Q mutation that decreases the $k_{cat}$ by $10^{4.7}$-fold and eliminates the pH dependence of the reaction (11). In the solution structure, a water that is proximal to Glu53 is positioned 4.2 Å away from the β-phosphorus and predicted to be the nucleophile (9). In the crystal structure the distance between Glu53 and the nucleophilic water is too large for deprotonation. However, the simultaneous decrease in water occupancy near Glu53 and appearance of the nucleophilic water in State 3 supports the possibility of Glu53-mediated deprotonation occurring prior to the water's moving from Glu53 to a new position of in-line, nucleophilic attack. The authors do not rule out alternative routes of deprotonation, which may occur by water molecules in the solvent or the γ-phosphate of 8-oxo-dGTP. However, proton density cannot be directly observed by X-ray crystallography at these resolutions, and sub-Ångström resolution or neutron crystallography are needed to provide a more direct way to visualize and verify the deprotonation of the nucleophilic water (23, 24).

This study demonstrates two important points. First, *in crystallo* catalysis and time-lapse crystallography are powerful tools for observations of how a reaction proceeds. The use of wild-type enzyme and biological substrate removes uncertainties arising from mutant enzymes or nonreactive analogs, which perturb both the active site and catalytic process. Second, the results show the ubiquity of the three-metal-ion mechanisms and ion trafficking in nucleic acid enzymes. Although the active sites of MutT and the previously characterized polymerases and nucleases differ, many of these enzymes require a third metal ion, usually $Mg^{2+}$ or $Mn^{2+}$, for catalysis. Interestingly, the third metal ion interacts with active-site residues of MutT, whereas the third metal does not contact active-site residues in DNA polymerase and RNase H (13–15, 17–21).

Overall, *in crystallo* studies are reshaping how we think about nucleic acid enzymes, whose active-site residues form a scaffold for metal-ion binding, and the metal ions are doing the hard work of driving catalysis by aligning substrates and stabilizing the negative charges formed during the reaction process. There are drawbacks and challenges to using the method. Crystals need to be readily reproducible, stable under reaction conditions, and diffract to a resolution that allows the detection of transient elements. Protons are not observable, and the time scale of cryo-crystallography is slower than the lifespan of a transition state. Thus, the appearance of a transition state, such as the pentacovalent phosphoanion intermediate that occurs in synthesis and hydrolyses reactions, is inferred from indirect studies and has not been directly observed using this method. Nevertheless, *in crystallo* catalysis has unequivocally illustrated the ubiquitous role of three metal ions in reactions formally known for two-metal ion catalysis.

1. A. S. Mildvan *et al.*, Structures and mechanisms of Nudix hydrolases. *Arch. Biochem. Biophys.* **433**, 129–143 (2005).
2. S. Waz *et al.*, Structural and kinetic studies of the human Nudix hydrolase MTH1 reveal the mechanism for its broad substrate specificity. *J. Biol. Chem.* **292**, 2785–2794 (2017).
3. J. A. Cowan, Metal activation of enzymes in nucleic acid biochemistry. *Chem. Rev.* **98**, 1067–1088 (1998).
4. T. A. Steitz, J. A. Steitz, A general two-metal-ion mechanism for catalytic RNA. *Proc. Natl. Acad. Sci. U.S.A.* **90**, 6498–6502 (1993).
5. C. M. Dupureur, One is enough: Insights into the two-metal ion nuclease mechanism from global analysis and computational studies. *Metallomics* **2**, 609–620 (2010).
6. F. Xie, S. H. Qureshi, G. A. Papadakos, C. M. Dupureur, One- and two-metal ion catalysis: Global single-turnover kinetic analysis of the PvuII endonuclease mechanism. *Biochemistry* **47**, 12540–12550 (2008).
7. W. Yang, J. Y. Lee, M. Nowotny, Making and breaking nucleic acids: Two-Mg2+-ion catalysis and substrate specificity. *Mol. Cell* **22**, 5–13 (2006).
8. T. Nakamura, Y. Yamagata, Visualization of mutagenic nucleotide processing by *Escherichia coli* MutT, a Nudix hydrolase. *Proc. Natl. Acad. Sci. U.S.A.* **119**, e2203118119 (2022).
9. C. Abeygunawardana *et al.*, Solution structure of the MutT enzyme, a nucleoside triphosphate pyrophosphohydrolase. *Biochemistry* **34**, 14997–15005 (1995).
10. T. Nakamura *et al.*, Structural and dynamic features of the MutT protein in the recognition of nucleotides with the mutagenic 8-oxoguanine base. *J. Biol. Chem.* **285**, 444–452 (2010).
11. T. K. Harris, G. Wu, M. A. Massiah, A. S. Mildvan, Mutational, kinetic, and NMR studies of the roles of conserved glutamate residues and of lysine-39 in the mechanism of the MutT pyrophosphohydrolase. *Biochemistry* **39**, 1655–1674 (2000).
12. N. L. Samara, Y. Gao, J. Wu, W. Yang, Detection of reaction intermediates in Mg$^{2+}$-dependent DNA synthesis and RNA degradation by time-resolved X-ray crystallography. *Methods Enzymol.* **592**, 283–327 (2017).
13. C. Chang, C. Lee Luo, Y. Gao, In crystallo observation of three metal ion promoted DNA polymerase misincorporation. *Nat. Commun.* **13**, 2346 (2022).
14. B. D. Freudenthal *et al.*, Uncovering the polymerase-induced cytotoxicity of an oxidized nucleotide. *Nature* **517**, 635–639 (2015).
15. B. D. Freudenthal, W. A. Beard, D. D. Shock, S. H. Wilson, Observing a DNA polymerase choose right from wrong. *Cell* **154**, 157–168 (2013).
16. R. Molina *et al.*, Visualizing phosphodiester-bond hydrolysis by an endonuclease. *Nat. Struct. Mol. Biol.* **22**, 65–72 (2015).
17. T. Nakamura, Y. Zhao, Y. Yamagata, Y. J. Hua, W. Yang, Watching DNA polymerase $\eta$ make a phosphodiester bond. *Nature* **487**, 196–201 (2012).
18. N. L. Samara, W. Yang, Cation trafficking propels RNA hydrolysis. *Nat. Struct. Mol. Biol.* **25**, 715–721 (2018).
19. R. Vyas, A. J. Reed, E. J. Tokarsky, Z. Suo, Viewing human DNA polymerase $\beta$ faithfully and unfaithfully bypass an oxidative lesion by time-dependent crystallography. *J. Am. Chem. Soc.* **137**, 5225–5230 (2015).
20. J. Wu, N. L. Samara, I. Kuraoka, W. Yang, Evolution of inosine-specific endonuclease V from bacterial DNase to eukaryotic RNase. *Mol. Cell* **76**, 44–56.e3 (2019).
21. W. Yang, P. J. Weng, Y. Gao, A new paradigm of DNA synthesis: Three-metal-ion catalysis. *Cell Biosci.* **6**, 51 (2016).
22. Y. Gao, W. Yang, Capture of a third Mg$^{2+}$ is essential for catalyzing DNA synthesis. *Science* **352**, 1334–1337 (2016).
23. N. Niimura, Neutrons expand the field of structural biology. *Curr. Opin. Struct. Biol.* **9**, 602–608 (1999).
24. H. Ogata, K. Nishikawa, W. Lubitz, Hydrogens detected by subatomic resolution protein crystallography in a [NiFe] hydrogenase. *Nature* **520**, 571–574 (2015).